

# Space-like dynamics in a reversible cellular automaton

K. Klobas\*, T. Prosen

Department of Physics, Faculty of Mathematics and Physics, University of Ljubljana,  
Ljubljana, Slovenia

\* katja.klobas@fmf.uni-lj.si

April 6, 2020

## Abstract

In this paper we study the space evolution in the *Rule 54 reversible cellular automaton*, which is a paradigmatic example of a deterministic interacting lattice gas. We show that the spatial translation of time configurations of the automaton is given in terms of local deterministic maps with the support that is small but bigger than that of the time evolution. The model is thus an example of space-time dual reversible cellular automaton, where the spatial evolution is configurationally constrained. We provide two equivalent interpretations of the result; the first one relies on the dynamics of quasi-particles and follows from an exhaustive check of all the relevant time configurations, while the second one relies on purely algebraic considerations based on the circuit representation of the dynamics. Additionally, we use the properties of the local space evolution maps to provide an alternative derivation of the matrix product representation of multi-time correlation functions of local observables positioned at the same spatial coordinate.

---

## Contents

|          |                                  |           |
|----------|----------------------------------|-----------|
| <b>1</b> | <b>Introduction</b>              | <b>2</b>  |
| <b>2</b> | <b>The model</b>                 | <b>4</b>  |
| 2.1      | Rule 54 dynamics                 | 4         |
| 2.2      | Macroscopic states               | 5         |
| 2.3      | Local observables                | 7         |
| 2.4      | Time states                      | 7         |
| <b>3</b> | <b>Space evolution</b>           | <b>8</b>  |
| <b>4</b> | <b>Circuit representation</b>    | <b>11</b> |
| 4.1      | The dual picture                 | 11        |
| 4.2      | Projected dual propagators       | 12        |
| 4.3      | Deterministic local 7-site gates | 13        |
| <b>5</b> | <b>Equilibrium time states</b>   | <b>14</b> |

|          |  |           |
|----------|--|-----------|
| 5.1      | Maximum entropy state  | 14        |
| 5.2      | Multi-time correlations for generic equilibrium states                         | 17        |
| 5.3      | Matrix product representation of the time state                                | 20        |
| <b>6</b> | <b>Conclusion</b>  | <b>21</b> |
| <b>A</b> | <b>Equivalence between the deterministic and nondeterministic dual gates</b>   | <b>22</b> |
| <b>B</b> | <b>Dual circuit representation of correlation functions</b>                    | <b>23</b> |
| <b>C</b> | <b>Factorization of the equilibrium state and the local few-site relations</b> | <b>24</b> |
| <b>D</b> | <b>Matrix-product form of multi-time correlation functions</b>                 | <b>25</b> |
|          | <b>References</b>  | <b>26</b> |

---

## 1 Introduction

Studying exactly solvable models has been traditionally a fruitful approach towards explaining the emergence of macroscopic phenomena from microscopies [1, 2]. In recent years, the many facets of integrability and solvability have been explored outside equilibrium physics [3]; for example, by studying long-time asymptotics of the initial value problem for a many-body interacting system — the so-called quenches [4], by developing generalized hydrodynamic description of integrable systems [5, 6], or by analysing random matrix models with intrinsic spatial locality structure — e.g. random local quantum circuits [7–10].

However, exact solutions of dynamical many-body problems for individual interacting systems are extremely scarce. A particularly interesting class of local quantum circuits that are exactly solvable in the statistical sense, yet they are not Bethe-ansatz or Yang-Baxter integrable, are *dual unitary* quantum circuits [11]. These are local interacting models in discrete space and discrete time where the roles of space and time can be exchanged while keeping dynamics unitary (a similar space-time duality has been explored in integrable field theories [12–14]). This property implies a nontrivial structure that enables exact computation of numerous physical quantities, such as local correlation functions [11, 15], entanglement spreading [16–18], operator entanglement [19, 20], and OTOCs [21]. However, dual unitarity restricts the growth of correlations to the maximal speed, which enforces strictly ballistic transport of conserved charges if present [11, 19]. Therefore these models cannot describe generic behaviour of systems with sub-ballistic transport of conserved quantities.

This motivates us to study the effect of exchanging time and space evolution in other 1+1 dimensional models, where the strict dual unitarity condition does not hold in hope of finding a generalized space-time duality allowing for potentially richer macroscopic physical properties, such as diffusive or super-diffusive transport. This question can be rephrased in the context of classical deterministic interacting lattice systems, where the property analogous to unitarity is the symplectic feature of the dynamical evolution law. An example of dual symplectic classical lattice dynamics that exhibits super-diffusive transport in the Kardar-Parisi-Zhang

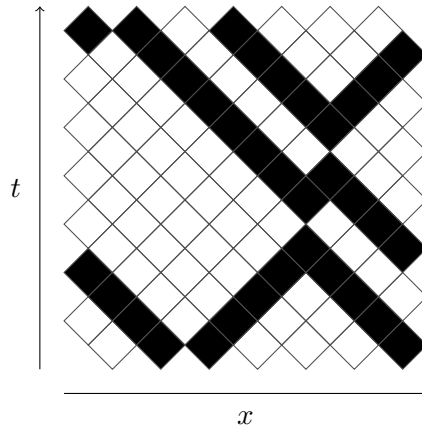


Figure 1: Example of RCA54 time evolution. The configuration at the bottom is evolved upwards according to the time evolution rules (2). Full sites (black rectangles) can be thought of as solitons that move with velocities  $\pm 1$  and scattering displaces them one site backwards. If the roles of space and time are exchanged, the dynamics can be still interpreted as solitons moving with velocities  $\pm 1$ , but when scattering their positions are moved one site *forward* with respect to the original trajectories.

universality class has been recently proposed [22, 23].

However, one can consider an even simpler class of interacting lattice systems where the local field variable takes only a discrete set of values, the so-called cellular automata. There, the feature analogous to symplecticity is the reversibility of dynamics, meaning that the local dynamical map over a discrete set of configurations is always one-to-one. A particularly interesting solvable example of such models is the Rule 54 reversible cellular automaton (RCA54) introduced by Bobenko et. al. in [24]<sup>1</sup> and studied extensively in the last years, both in classical [26–31] and in quantum setting [32–35]. In particular, dynamical structure factor of this model has been computed exactly [30] and shown to exhibit diffusive transport.

We argue that RCA54 is an excellent candidate for studying deterministic space evolution. Indeed, a recent study revealed that probability distributions of time configurations exhibit an efficient matrix-product description [31], suggesting that translating a given time configuration in space might be given by a composition of deterministic maps with a finite support. Another indication that a reversible space evolution formulation of RCA54 should be possible comes from the quasi-particle interpretation of the dynamics; RCA54 rules describe solitons (kinks) that move with fixed velocities and interact pairwise acquiring a delay for one site after each scattering. Exchanging the roles of space and time results in similar dynamics, the only difference is that the scattering now moves the solitons one site forward with respect to the original trajectory. See Figure 1 for a representative example.

In the paper we put this intuitive picture on formal grounds by expressing the space evolution in terms of local deterministic maps, i.e. again as a reversible cellular automaton. In Section 2 we define the model and introduce the statistical states and observables. In Section 3 we construct the local space evolution rules. We demonstrate that the space evolution is indeed local and deterministic, but it has to be defined on a reduced configuration space since not all of the configurations can be realized in the time evolution. Therefore, the

<sup>1</sup>An equivalent model is also known as ERCA 250R in the classification introduced by Takesue [25].

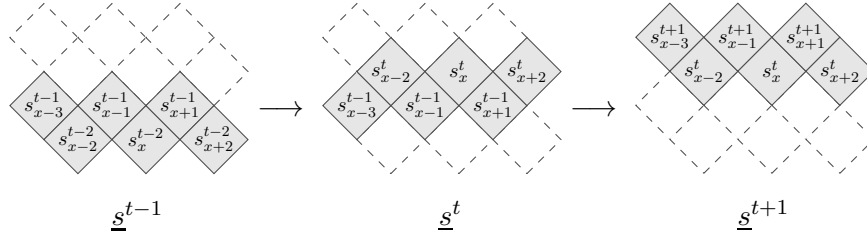


Figure 2: Schematic representation of the lattice geometry and time evolution. At every time step, half of the sites are updated as expressed in (3). The new value depends on the values of the three consecutive sites as described in (2).

corresponding spatial cellular automaton is configurationally constrained. Furthermore, the map implementing the space evolution has a larger support than the local time evolution map. In Section 4 we provide an alternative view of the problem by recasting the dynamics in terms of reversible logical circuits with three-site gates. This allows us to express the space evolution in an equivalent but simpler way. In Section 5 we use the circuit representation to find an alternative construction of *time-states* (as introduced in [31]) that does not explicitly depend on the quasi-particle interpretation. Finally, Section 6 contains some closing remarks.

## 2 The model

### 2.1 Rule 54 dynamics

The model is defined on a one-dimensional zig-zag lattice of even length  $2n$  with each site being either occupied or empty. A configuration at time  $t$  is given as a string of  $2n$  binary digits,  $\underline{s}^t = (\dots, s_x^t, s_{x+1}^{t-1}, s_{x+2}^t, \dots)$ , where the subscript denotes the position coordinate along the chain, superscript is the time coordinate and the time and space coordinates have the same parity,  $x + t \equiv 0 \pmod{2}$ . Explicitly,

$$\underline{s}^{2t} = (s_1^{2t-1}, s_2^{2t}, s_3^{2t-1}, \dots, s_{2n}^{2t}), \quad \underline{s}^{2t+1} = (s_1^{2t+1}, s_2^{2t}, s_3^{2t+1}, \dots, s_{2n}^{2t}), \quad (1)$$

where  $s_x^t = 1$  represents an occupied site and  $s_x^t = 0$  an empty one. The time evolution is defined in discrete time and it is characterized by a local three site update rule that changes the value of the middle bit (site) depending on the configuration of the triple of neighbouring sites,

$$s_2' = \chi(s_1, s_2, s_3) = s_1 + s_2 + s_3 + s_1 s_3 \pmod{2}. \quad (2)$$

At every time step, the bits with the smaller time label are updated,

$$s_x^{t+1} = \chi(s_{x-1}^t, s_x^{t-1}, s_{x+1}^t), \quad (3)$$

where the *periodic boundaries* are assumed,  $s_{2n+1}^t \equiv s_1^t$ . Geometrically, the time evolution can be imagined to update the bottom sites of the zig-zag chain upwards while the previous top sites become the bottom sites of the propagated chain corresponding to the new time step, as schematically shown in Figure 2. Using this convention, the local time evolution rule (2) can



with  $U_k$  being the shorthand notation for the local operator  $U$  that acts nontrivially on the sites  $(k-1, k, k+1)$ ,

$$U_k \equiv \mathbb{1}^{\otimes k-2} \otimes U \otimes \mathbb{1}^{\otimes 2n-k-1}. \quad (9)$$

A distinguished set of statistical states are *the stationary states*, which are invariant under the time evolution. Due to the staggering, we require these states to map into themselves after *even* time steps and therefore each stationary state is associated with two vectors,  $\mathbf{p}$  and  $\mathbf{p}'$ , corresponding to even and odd time steps respectively,

$$\mathbf{p}' = U^e \mathbf{p}, \quad \mathbf{p} = U^o \mathbf{p}'. \quad (10)$$

A simple class of 2-parameter stationary states, similar to the non-equilibrium stationary states introduced in [28, 29], can be expressed in a matrix product form,

$$\mathbf{p}(\xi, \omega) = \frac{1}{Z_{2n}(\xi, \omega)} \text{tr} \left( \mathbf{W}_1(\xi, \omega) \mathbf{W}'_2(\xi, \omega) \mathbf{W}_3(\xi, \omega) \cdots \mathbf{W}'_{2n}(\xi, \omega) \right), \quad (11)$$

where  $\mathbf{W}^{(l)}(\xi, \omega) = [W_0^{(l)}(\xi, \omega), W_1^{(l)}(\xi, \omega)]^T$ , are vectors of matrices and the subscripts refer to the positions of physical sites. Here, the auxiliary space is 3-dimensional, with the matrices taking the following form,

$$W_0(\xi, \omega) = W'_0(\omega, \xi) = \begin{bmatrix} 1 & 0 & 0 \\ \xi & 0 & 0 \\ 1 & 0 & 0 \end{bmatrix}, \quad W_1(\xi, \omega) = W'_1(\omega, \xi) = \begin{bmatrix} 0 & \xi & 0 \\ 0 & 0 & 1 \\ 0 & 0 & \omega \end{bmatrix}, \quad (12)$$

and the normalization is given by

$$Z_{2n}(\xi, \omega) = \text{tr} \left( (W_0(\xi, \omega) + W_1(\xi, \omega))(W'_0(\xi, \omega) + W'_1(\xi, \omega)) \right)^n. \quad (13)$$

To lighten the notation, when not ambiguous, we will suppress the explicit dependence on the spectral parameters  $\xi, \omega$ .

The matrices  $\mathbf{W}, \mathbf{W}'$  fulfill the following cubic algebraic relation,

$$U \mathbf{W}_1 \mathbf{W}'_2 \mathbf{W}_3 S = \mathbf{W}_1 S \mathbf{W}_2 \mathbf{W}'_3, \quad (14)$$

which can be equivalently expressed in physical space components as

$$W_{s_1} W'_{\chi(s_1, s_2, s_3)} W_{s_3} S = W_{s_1} S W_{s_2} W'_{s_3}. \quad (15)$$

Here we introduced the *delimiter matrix*  $S$  acting on the auxiliary space,

$$S = \begin{bmatrix} 1 & 0 & 0 \\ 0 & 0 & 1 \\ 0 & 1 & 0 \end{bmatrix}, \quad S^2 = \mathbb{1}. \quad (16)$$

Defining the odd-time version of the matrix product state (11) by exchanging the roles of  $\mathbf{W}$  and  $\mathbf{W}'$ ,

$$\mathbf{p}' = \frac{1}{Z_{2n}} \text{tr} \left( \mathbf{W}'_1 \mathbf{W}_2 \mathbf{W}'_3 \cdots \mathbf{W}_{2n} \right), \quad (17)$$

time invariance condition (10) follows directly from the cubic relation (14) and the fact that the local time evolution operator  $U$  and matrix  $S$  are *involutory*, i.e.  $U = U^{-1}$  and  $S = S^{-1}$ .

### 2.3 Local observables

Observables are real valued functions over the configuration space and form a commutative algebra,

$$\mathcal{A}, \mathcal{B} : \mathbb{Z}_2^{2n} \rightarrow \mathbb{R}, \quad (\mathcal{A}\mathcal{B})(\underline{s}) = \mathcal{A}(\underline{s})\mathcal{B}(\underline{s}). \quad (18)$$

The space of observables can be thought of as a vector space that is dual to the space of macroscopic states (probability vectors)  $\mathbf{p}$ . It is possible to define time evolution of observables via the following explicit expression of expectation values,

$$\langle \mathcal{A}(t) \rangle_{\mathbf{p}} = \sum_{\underline{s}^0} \mathcal{A}(\underline{s}^t) p_{\underline{s}^0}. \quad (19)$$

In the paper, however, we will mostly deal with *one-site observables*, which only depend on the configuration at one site,  $\mathcal{A}_x(\underline{s}) = a(s_x)$ , where  $a$  is a real valued function from the one-site configuration space,  $a : \mathbb{Z}_2 \rightarrow \mathbb{R}$ . Therefore, the expectation value of  $a$  at site  $x$  and time  $t$  takes the following form,

$$\langle a(x, t) \rangle_{\mathbf{p}} = \sum_{\underline{s}^0} p_{\underline{s}^0} a(s_x^t). \quad (20)$$

This expression can be also interpreted as an inner product by introducing a one-site (unnormalized) maximum entropy vector  $\boldsymbol{\omega}$  and a diagonal matrix representation of the observable,

$$\boldsymbol{\omega} = [1 \quad 1], \quad \mathcal{O}_x(a) = \mathbb{1}^{\otimes x-1} \otimes \begin{bmatrix} a(0) & 0 \\ 0 & a(1) \end{bmatrix} \otimes \mathbb{1}^{\otimes 2n-x}. \quad (21)$$

Using this notation, the expectation values (20) can be expressed as

$$\langle a(x, t) \rangle_{\mathbf{p}} = \boldsymbol{\omega}^{\otimes 2n} \mathcal{O}_x(a) \mathbf{p}(t). \quad (22)$$

### 2.4 Time states

We proceed to define *time configurations* as configurations of empty/full sites observed at the same position  $x$  and different times  $t$ , e.g. configurations of vertical zig-zag shaped chains from Figure 1. Analogously to (1), time configurations  $\underline{s}_x$  are bit sequences

$$(\dots, s_x^{t-2}, s_x^{t-1}, s_x^t, s_x^{t+1}, \dots), \quad (23)$$

where the space and time label have the same parity,  $x + t \equiv 0 \pmod{2}$ . Explicitly,

$$\underline{s}_{2x} = (s_{2x-1}^1, s_{2x}^2, s_{2x-1}^3, \dots, s_{2x}^{2m}), \quad \underline{s}_{2x+1} = (s_{2x+1}^1, s_{2x}^2, s_{2x+1}^3, \dots, s_{2x}^{2m}). \quad (24)$$

For simplicity we assume that the time label  $t$  takes the values in a finite range between 1 and  $2m$ . In analogy with the statistical states, *time states* are probability distributions over the space of time configurations and can be represented as vectors from  $\mathbb{R}^{2^{2m}}$ ,

$$\mathbf{q} = [q_0 \quad q_1 \quad q_2 \quad \dots \quad q_{2^{2m}-1}]^T, \quad \sum_{s=0}^{2^{2m}-1} q_s = 1, \quad (25)$$

where each component  $q_s \geq 0$  corresponds to the probability of the time configuration given by the binary representation of  $s$ .

However, not every string of  $2m$  binary digits represents a valid time configuration. In particular, the rules (4) imply that in a time configuration full sites always come in pairs, while three consecutive full sites are forbidden. Therefore it makes sense to restrict the discussion only to *allowed* (also referred to as *accessible*) time configurations, where no substrings  $(1, 1, 1)$  or  $(0, 1, 0)$  appear. Accordingly, the only nonzero components of time states should correspond to allowed configurations. This is equivalent to requiring the time states to be invariant under the action of local projectors  $P_k$ ,

$$P_k \mathbf{q} = \mathbf{q}, \quad P_k \equiv \mathbb{1}^{\otimes k-2} \otimes P \otimes \mathbb{1}^{\otimes 2m-k-1}, \quad (26)$$

where  $P$  is the 3 site projector to the allowed subspace of states,

$$P_{(s'_1, s'_2, s'_3), (s_1, s_2, s_3)} = \delta_{s'_1, s_1} \delta_{s'_2, s_2} \delta_{s'_3, s_3} (1 - \delta_{s_1, s_3} \delta_{s_2, 1}). \quad (27)$$

In analogy with stationary states one can define *equilibrium time-states*. These states correspond to probability distributions of time configurations observed under the assumption of the system being in the equilibrium state  $\mathbf{p}$  as introduced by Eq. (11). Explicitly, the equilibrium time-states are uniquely determined by the expectation values of *multi-time correlation functions* of one-site observables at the same position,<sup>3</sup>  $C_{a_1, a_2, \dots, a_{2m}}(\mathbf{p}) = \lim_{n \rightarrow \infty} C_{a_1, a_2, \dots, a_{2m}}^{(2n)}(\mathbf{p})$ , defined as the large system size limit of the following correlation function,

$$C_{a_1, a_2, a_3, \dots, a_{2m}}^{(2n)}(\mathbf{p}) = \langle a_1(n^*, 0) a_2(n^* + 1, 1) a_3(n^*, 2) \cdots a_{2m}(n^* + 1, 2m - 1) \rangle_{\mathbf{p}}, \quad (28)$$

where  $n^* = 2 \lfloor \frac{n}{2} \rfloor$ ,

i.e.  $n^* = n$  for even  $n$  and  $n^* = n - 1$  for odd  $n$ . By definition (22), the correlation function can therefore be recast as the following inner product between the vector  $\boldsymbol{\omega}^{\otimes 2n}$  and the equilibrium distribution vector  $\mathbf{p}$  on which the appropriate sequential product of time evolution operators  $U^{e/o}$  and matrix representations of local observables  $\mathcal{O}_{n^*/n^*+1}(a_j)$  is applied,

$$C_{a_1, a_2, a_3, \dots, a_{2m}}^{(2n)}(\mathbf{p}) = \boldsymbol{\omega}^{\otimes 2n} \mathcal{O}_{n^*+1}(a_{2m}) U^e \cdots U^e \mathcal{O}_{n^*}(a_3) U^o \mathcal{O}_{n^*+1}(a_2) U^e \mathcal{O}_{n^*}(a_1) \mathbf{p}. \quad (29)$$

The equilibrium time state  $\mathbf{q}$  is determined as the probability distribution that uniquely fixes all the values of multi-time correlation functions  $C_{a_1, a_2, \dots, a_{2m}}(\mathbf{p})$ ,

$$C_{a_1, a_2, \dots, a_{2m}} = \sum_{s_1, s_2, \dots, s_{2m}} q_{s_1 s_2 \dots s_{2m}} \prod_j^{2m} a_j(s_j) = \boldsymbol{\omega}^{\otimes 2m} \mathcal{O}_{2m}(a_{2m}) \cdots \mathcal{O}_2(a_2) \mathcal{O}_1(a_1) \mathbf{q}, \quad (30)$$

where the first equality follows from the definition and the second equality is just the convenient vectorial representation. As was shown in Ref. [31], these equilibrium time-states exhibit a simple matrix product representation.

### 3 Space evolution

Our goal is to express the evolution of time configurations in the space direction as schematically shown in Figure 3. In general, there is no guarantee that the space evolution can be

<sup>3</sup>Due to the geometry of the problem, the observables are technically positioned at one of the two neighbouring sites, depending on the parity of the time-step.



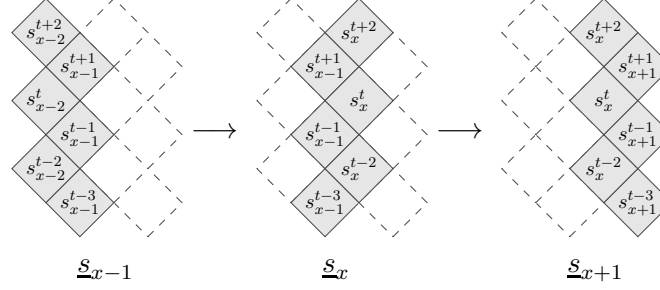


Figure 3: Illustration of the geometry of space evolution. In analogy with the time evolution shown in Figure 2, at every step the bits with the smaller space label deterministically change, while the others stay the same.

expressed as a composition of local deterministic maps. In our case, however, we expect this to be the case due to the soliton description of the model: the dynamics in the space direction can be understood as particles moving either upwards or downwards with velocity 1. When two oppositely moving particles meet, they get displaced one site forward with respect to their original trajectories, mimicking repulsive interaction. This suggests the existence of a deterministic local map,

$$s_{x+1}^t = \phi(s_{x/x-1}^{t-r}, \dots, s_{x-1}^{t-2}, s_x^{t-1}, s_{x-1}^t, s_x^{t+1}, s_{x-1}^{t+2}, \dots, s_{x/x-1}^{t+r}), \quad (31)$$

where  $r \in \mathbb{N}$  characterizes the support (of size  $2r + 1$ ) of the map.

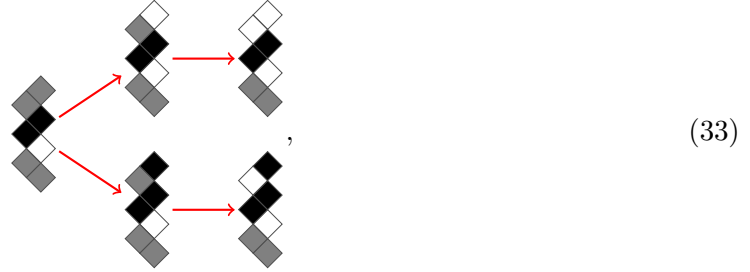
The time evolution diagrams (4) immediately imply that local space propagators cannot be expressed in terms of maps with support 3 (i.e.  $r = 1$ ). Indeed, it is easy to see that the closest two neighbouring sites do not encode enough information to deterministically propagate the state in space. In particular, the last two pairs of diagrams have the same configurations of the left three bits and different values of the right site. Therefore, the support must be larger. Note that we additionally have to require that the local space maps shifted by an even number of sites commute, i.e. the order in which we apply (31) on a given time configuration should not matter.

It is easy to see that the support 7 (i.e.  $r = 3$ ) suffices to express the deterministic space propagation rules. We start by observing that the first four of the diagrams (4) give the 3-site deterministic mapping also in the space direction,

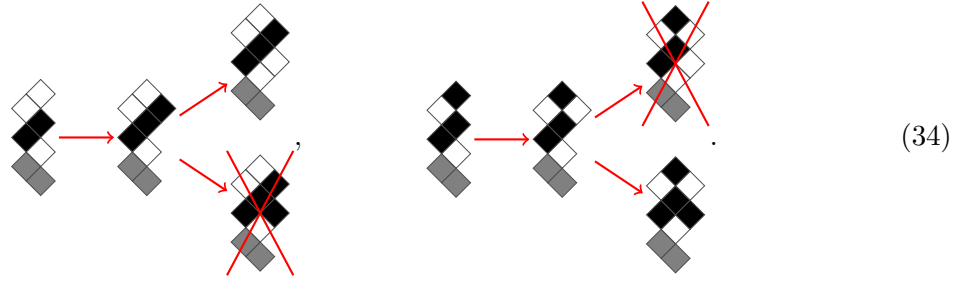
(32)

Now let us consider the subconfiguration  $(0, 1, 1)$ , which does not have a unique 3-site mapping and we add neighbouring sites. By avoiding the forbidden subconfigurations, there are only two possibilities of how the configuration can continue to the top; either  $(0, 1, 1, 0, 0)$  or

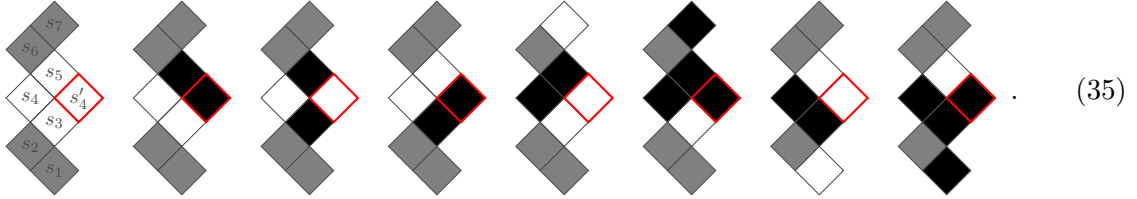
$(0, 1, 1, 0, 1)$ , which can be explicitly visualised as



where the gray squares represent the sites with unknown or undetermined states. The top three sites in both configurations can be uniquely evolved by the 3-site local maps (32). After applying these deterministic rules we try to update the central bit to value 0 or 1, while at the same requiring that the updated configuration does not violate the time-configuration restriction (26). We are left with a unique updated value for the central bit



This provides the deterministic mapping corresponding to 5th and 6th diagram of the time evolution rules (4), and by flipping the diagrams upside down, we obtain the last two rules. Together with the simple 3-site rules (32), this completes the construction of local deterministic space evolution maps,



Explicitly, the rules can be expressed as

$$\phi(s_1, s_2, s_3, s_4, s_5, s_6, s_7) = \begin{cases} 0; & s_3 = s_4 = s_5 = 0, \\ 1; & s_3 = s_4 = 0, s_5 = 1, \\ 0; & s_3 = 0, s_4 = s_5 = 1, s_7 = 0, \\ 1; & s_3 = 0, s_4 = s_5 = 1, s_7 = 1, \\ 1; & s_3 = 1, s_4 = s_5 = 0, \\ 0; & s_3 = 1, s_4 = 0, s_5 = 1, \\ 0; & s_1 = 0, s_3 = s_4 = 1, s_5 = 0, \\ 1; & s_1 = 1, s_3 = s_4 = 1, s_5 = 0. \end{cases} \quad (36)$$

The update rules  $s'_4 = \phi(s_1, s_2, s_3, s_4, s_5, s_6, s_7)$  do not depend explicitly on the values of the sites  $s_2$  and  $s_6$ , therefore all the local maps applied at the same step commute.





which follows directly from the definition of  $\tilde{U}^{e/o}$  (47) and the commutativity of local projectors centered at different sites. This equality can be visualised graphically, by first introducing the following representation for the projector  $P$ ,

$$\begin{array}{c} s_1 - \bullet - s'_1 \\ s_2 - \bullet - s'_2 \\ s_3 - \bullet - s'_3 \end{array}, \quad (49)$$

and transforming the diagram (40) as

$$\hat{U}^o \hat{U}^e \hat{U}^o \rightarrow \hat{U}^o \hat{U}^e \hat{U}^o \rightarrow \hat{U}^o P^o P^e \hat{U}^e P^e P^o \hat{U}^o \rightarrow \hat{U}^e \quad (50)$$

where we took into account the fact that the only combinations of noncommuting gates are the ones with the big circle of one gate sitting on the same line as the small circle of another one. Explicitly, in this case the following 3 pairs *do not* commute,

$$\begin{array}{ccc} \begin{array}{c} \bullet \\ \bullet \\ \bullet \\ \bullet \end{array} \neq \begin{array}{c} \bullet \\ \bullet \\ \bullet \\ \bullet \end{array}, & \begin{array}{c} \bullet \\ \bullet \\ \bullet \\ \bullet \end{array} \neq \begin{array}{c} \bullet \\ \bullet \\ \bullet \\ \bullet \end{array}, & \begin{array}{c} \bullet \\ \bullet \\ \bullet \\ \bullet \end{array} \neq \begin{array}{c} \bullet \\ \bullet \\ \bullet \\ \bullet \end{array}. \end{array} \quad (51)$$

### 4.3 Deterministic local 7-site gates

The one-step space evolution operators  $\tilde{U}^{e/o}$  can be written as products of local gates with support 7 that are deterministic on the reduced configuration subspace, i.e. it is possible to suitably define local propagators  $\tilde{V}$  and  $\tilde{W}$  so that  $\tilde{U}^{o/e}$  take the following form,

$$\begin{aligned} \tilde{U}^e &= \left( \prod_t \tilde{W}_{8t+10} \right) \left( \prod_t \tilde{W}_{8t+6} \right) \left( \prod_t \tilde{V}_{8t+8} \right) \left( \prod_t \tilde{V}_{8t+4} \right), \\ \tilde{U}^o &= \left( \prod_t \tilde{W}_{8t+11} \right) \left( \prod_t \tilde{W}_{8t+7} \right) \left( \prod_t \tilde{V}_{8t+9} \right) \left( \prod_t \tilde{V}_{8t+5} \right), \end{aligned} \quad (52)$$

where the subscript denotes the middle site of the subchain on which the local evolution operators acts, i.e.  $\tilde{W}_t$  acts nontrivially on the sites  $t-3$ ,  $t-2$ ,  $t-1$ ,  $t$ ,  $t+1$ ,  $t+2$  and  $t+3$ .

Graphically, this is represented by the following diagram,

$$(53)$$

The operators  $\tilde{V}$ ,  $\tilde{W}$  can be explicitly written in terms of the dual 3-site operators  $\hat{U}$  by introducing the following 5-site projector  $Q$ ,

$$Q_{(s'_1, s'_2, s'_3, s'_4, s'_5), (s_1, s_2, s_3, s_4, s_5)} = \delta_{s_1, s'_1} \delta_{s_2, s'_2} \delta_{s_3, s'_3} \delta_{s_4, s'_4} \delta_{s_5, s'_5} \cdot (1 - \delta_{s_2, 0} \delta_{s_3, 1} \delta_{s_1 + s_4, 1}) (1 - \delta_{s_4, 0} \delta_{s_3, 1} \delta_{s_2 + s_5, 1}). \quad (54)$$

Then the 7-site gates can be expressed as a 3-site projected operator  $\hat{U}$ , sandwiched between two  $P$  projectors on one and two  $Q$  projectors on the other side,

$$(55)$$

or equivalently

$$\tilde{V}_t = Q_{t+1} Q_{t-1} \tilde{U}_t P_{t+1} P_{t-1}, \quad \tilde{W}_t = P_{t+1} P_{t-1} \tilde{U}_t Q_{t+1} Q_{t-1}. \quad (56)$$

These gates are deterministic on the restricted space of allowed time-configurations, since the following holds,

$$\tilde{V}_t \tilde{V}_t^T = \tilde{W}_t^T \tilde{W}_t = Q_{t-1} P_t Q_{t+1}, \quad \tilde{V}_t^T \tilde{V}_t = \tilde{W}_t \tilde{W}_t^T = P_{t-1} P_t P_{t+1}, \quad (57)$$

where right-hand-sides are diagonal projection matrices with matrix elements that can only be 0 or 1. Therefore, to see that the space evolution is local and deterministic, we only have to show that the diagrams (53) and (50) are equivalent. The proof is provided in Appendix A.

## 5 Equilibrium time states

### 5.1 Maximum entropy state

Similar ideas can be employed to find equilibrium time-states, i.e. the probability distributions of time-configurations under the assumption of the underlying system being in equilibrium (or



on the middle site.<sup>4</sup> In our case the dual propagation is deterministic as well, therefore, in analogy to dual unitary circuits [11], we expect the diagram to further simplify. However, since the definition of local deterministic gates is rather involved (see Eq. (55)), the deterministic property cannot be directly used to reduce the diagram (60). Instead, we take advantage of the following two diagrammatic relations fulfilled by  $\hat{U}$ ,

$$(61)$$

We stress that even though these diagrams are conceptually similar to those used to prove the deterministic property of space evolution (cf. (92)), the precise relation between the two is not clear at present.

Because of  $\hat{U}^T = \hat{U}$ , also the left-right reversed diagrams hold. Additionally, since the observables are diagonal, they all commute with the three-site projector  $P$ . This, together with the relations (61), allows us to transform the correlation function  $C_{a_1, a_2, \dots, a_{2m}}(\mathbf{p}_\infty)$  into a diagram with only the two inner-most layers of dual gates left,

$$C_{a_1, a_2, a_3, \dots, a_{2m}}(\mathbf{p}_\infty) = 2^{-2m} \quad (62)$$

This can be put in a more convenient form by introducing left and right edge matrix product states,  $(L|\mathbf{A}_1\mathbf{B}'_2\mathbf{A}_3 \cdots \mathbf{A}_{2m-1}|R)$  and  $(L|\mathbf{A}_2\mathbf{B}_3\mathbf{A}_4 \cdots \mathbf{A}_{2m}|R)$ , to replace the two remaining dual gate layers. The auxiliary space is 2-dimensional, with the following boundary vectors

$$\perp \equiv (L| = [1 \quad 1], \quad \top \equiv |R) = \begin{bmatrix} 1 \\ 1 \end{bmatrix}. \quad (63)$$

The matrices  $A_s$  are diagonal with one nonzero entry,

$$\star \equiv \mathbf{A} \equiv \star, \quad A_0 = \begin{bmatrix} 1 & 0 \\ 0 & 0 \end{bmatrix}, \quad A_1 = \begin{bmatrix} 0 & 0 \\ 0 & 1 \end{bmatrix}, \quad (64)$$

while the matrix elements of  $B_s, B'_s$ , diagrammatically represented by the squares

$$\blacksquare \equiv \mathbf{B}, \quad \blacksquare \equiv \mathbf{B}', \quad B_0 = B'_0 = \begin{bmatrix} 1 & 1 \\ 1 & 1 \end{bmatrix}, \quad B_1 = B'_1 = \begin{bmatrix} 0 & 2 \\ 2 & 0 \end{bmatrix}, \quad (65)$$

<sup>4</sup>To be more precise, the exact requirement is the validity of (59), which is satisfied by any bistochastic matrix.



are determined by requiring the following relations,

$$(66)$$

Note that the first pair of diagrams follows from the second one due to  $(L|A_0|R) = (L|A_1|R) = 1$ . The correlation function can finally be rewritten as

$$C_{a_1, a_2, a_3, \dots, a_{2m}}(\mathbf{p}_\infty) = 2^{-2m} \dots (67)$$

The matrix-product-state (MPS) form of the time-state follows directly from here. However, before showing it explicitly, we first generalize the result to the class of equilibrium states  $\mathbf{p}$ , introduced in section 2.2.

## 5.2 Multi-time correlations for generic equilibrium states

To conveniently express multi-time correlations for the class of states  $\mathbf{p}$  that can be expressed in a matrix product form (11), we introduce the diagrammatic notation for the MPS,

$$\mathbf{W} \equiv \blacktriangleleft, \quad \mathbf{W}' \equiv \blacktriangleright, \quad \mathbf{S} \equiv \blacksquare, (68)$$

which allows us to diagrammatically express finite-size correlation function as,

$$C_{a_1, a_2, a_3, \dots, a_{2m}}^{(2n)}(\mathbf{p}) = \frac{1}{Z_{2n}} \dots (69)$$

Similarly to the case of the maximum entropy state, the deterministic time evolution implies that the gates outside of the light-cone can be removed. To prove this, in addition to (59), we use the following three-site algebraic relations fulfilled by the state  $\mathbf{p}$ ,

$$(70)$$



while the matrices  $B_s$  fulfill the analogous identities for the right edge,

$$(77)$$

The solution to these relations can be explicitly expressed in terms of tensors  $\alpha_{s_1 s_2 s_3}$ ,  $\alpha'_{s_1 s_2 s_3}$  as

$$B_0 = \begin{bmatrix} \alpha_{000} & \alpha_{001} \\ \alpha_{000} & \alpha_{001} \end{bmatrix}, \quad B_1 = \begin{bmatrix} 0 & \alpha_{000} + \alpha_{001} \\ \alpha_{000} + \alpha_{001} & 0 \end{bmatrix},$$

$$B'_0 = \begin{bmatrix} \alpha'_{000} & \alpha'_{100} \\ \alpha'_{000} & \alpha'_{100} \end{bmatrix}, \quad B'_1 = \begin{bmatrix} 0 & \alpha'_{000} + \alpha'_{100} \\ \alpha'_{000} + \alpha'_{100} & 0 \end{bmatrix}.$$

$$(78)$$

Additional details and the explicit values of the coefficient tensors are provided in Appendix C.

Using the relations (76) and (77), together with the observation that  $\langle L|A_s|R \rangle = 1$  for any  $s$ , namely

$$\overline{\text{X}} \equiv \bullet, \quad \overline{\text{X}} \equiv \bullet, \quad (79)$$

the layers of dual gates in the diagram (74) can be removed one after another, until we are left with the innermost two layers squeezed between two vertical matrix product states,

$$C_{a_1, a_2, a_3, \dots, a_{2m}}(\mathbf{p}) = \frac{\lambda^{-m}}{\langle l|r \rangle} \text{Diagram} \quad (80)$$

To remove the last two layers, we note that the observables commute with all the projectors since they are diagonal in the same basis and structure of  $\mathbf{B}$ ,  $\mathbf{B}'$  implies that left (right) vertical states are invariant under projectors centered at odd (even) sites,

$$(81)$$

Additionally we have

$$(82)$$

These relations are analogous to the right-most diagrams from (76) and (77), and imply that the multi-time correlation function can be finally written as follows

$$C_{a_1, a_2, a_3, \dots, a_{2m}}(\mathbf{p}) = \frac{\lambda^{-m}}{\langle l|r \rangle} \begin{array}{c} \text{Diagram 1} \\ \vdots \\ \text{Diagram 2} \end{array} \quad (83)$$

In components Eq. (83) reads as

$$C_{a_1, \dots, a_{2m}} = \sum_{s_1, s_2, s_3, \dots, s_{2m}} \frac{\langle l|W'_{s_1}W_{s_2}|r \rangle}{\lambda^k \langle l|r \rangle} (L|A_{s_1}B'_{s_2} \cdots A_{s_{2m-1}}|R) \prod_{j=1}^{2m} a_j(s_j) (L|A_{s_2}B_{s_3} \cdots A_{s_{2m}}|R). \quad (84)$$

### 5.3 Matrix product representation of the time state

The above results can be expressed in terms of a time state, as defined in Section 2.4. The equilibrium time state  $\mathbf{q} \in \mathbb{R}^{2^{2m}}$  corresponding to the equilibrium state  $\mathbf{p}$  uniquely fixes multi-time correlation functions, which by definition implies

$$C_{a_1, a_2, a_3, \dots, a_{2m}} = \sum_{s_1, s_2, s_3, \dots, s_{2m}} q_{s_1 s_2 s_3 \dots s_{2m}} \prod_{j=1}^{2m} a_j(s_j). \quad (85)$$

We can then read the probabilities of time-configurations  $q_{s_1 s_2 \dots s_{2m}}$  directly from (84) as

$$q_{s_1 s_2 s_3 \dots s_{2m}} = \frac{\langle l|W'_{s_1}W_{s_2}|r \rangle}{\lambda^k \langle l|r \rangle} (L|A_{s_1}B'_{s_2}A_{s_3} \cdots A_{s_{2m-1}}|R) (L|A_{s_2}B_{s_3}A_{s_4} \cdots A_{s_{2m}}|R). \quad (86)$$

From here, an MPS representation is obtained by introducing matrices  $\tilde{A}_s, \tilde{A}'_s$  that act on the 4-dimensional auxiliary space as

$$\tilde{A}_s = A_s \otimes B_s, \quad \tilde{A}'_s = B'_s \otimes A_s, \quad (87)$$

and defining boundary vectors  $|\tilde{R}\rangle, \langle \tilde{L}|$  as the solutions to the following relations,

$$\begin{aligned} \langle \tilde{L}|\tilde{A}_{s_1}\tilde{A}'_{s_2} &= \frac{\langle l|W'_{s_1}W_{s_2}|r \rangle}{\langle l|r \rangle} \left( (L|A_{s_1}B'_{s_2}) \otimes ((L|A_{s_2}), \right. \\ \tilde{A}_{s_1}\tilde{A}'_{s_2}|\tilde{R}\rangle) &= \left( A_{s_1}|R) \right) \otimes \left( B_{s_1}A_{s_2}|R) \right). \end{aligned} \quad (88)$$

The time-state can thus be written in the matrix product form as

$$\mathbf{q} = \frac{1}{\lambda^k} \langle \tilde{L}|\tilde{\mathbf{A}}_1\tilde{\mathbf{A}}'_2\tilde{\mathbf{A}}_3 \cdots \tilde{\mathbf{A}}'_{2m}|\tilde{R}\rangle. \quad (89)$$

As shown in Appendix D, this form of the time-state is equivalent to the MPS introduced in [31].

## 6 Conclusion

In this paper we have studied the properties of space evolution in Rule 54 reversible cellular automaton. We have shown that space translation of time configurations (i.e. configurations at the same position in the time direction) can be formulated as a reversible cellular automaton. In other words, the spatial dynamics can be expressed in terms of local deterministic maps with finite support. We have provided two different interpretations of local space evolution; as 7-site local deterministic maps, or equivalently, as a composition of non-deterministic 3-site gates and 3-site projectors onto the subspace of allowed configurations.

The result is interesting from two different points of view. On one hand, due to the existence of time states, the space dynamics of RCA54 can be studied as a novel solvable deterministic interacting model, where quasi-particles move with fixed velocities  $\pm 1$  and undergo pairwise scattering. The main difference with respect to the usual (temporal) dynamics in RCA54 is the nature of two-body interaction, which speeds the particles up instead of slowing them down, i.e. it is repulsive rather than attractive. Arguably the more interesting perspective is to use the properties of the space dynamics to express nontrivial dynamical physical quantities. We have demonstrated this approach can be fruitful by finding an alternative derivation of the MPS form of *equilibrium time-states*, i.e. probability distributions that uniquely determine multi-time correlation functions at the same position.

The paper opens several interesting open questions. For instance, what is limit of this approach? It would be interesting to see whether the circuit picture can provide a new perspective on two-point spatio-temporal correlation functions [30] or time evolution of density matrices in the quantum version of the model [35]. This would provide a new perspective that does not explicitly rely on the quasi-particle interpretation of the dynamics, and is hence more robust and easier to generalize. Furthermore, one would like to understand whether RCA54 is an isolated example or it belongs to the bigger class of *dual reversible* cellular automata with a different but finite support of local evolution maps in space and time directions. Such a class would provide a generalization of dual unitary models [11] which could support richer transport properties, while many results would still be obtained exactly.

## Acknowledgements

KK thanks Bruno Bertini for insightful discussions and valuable comments on the manuscript.

**Funding Information** This work has been supported by the European Research Council under the Advanced Grant No. 694544 – OMNES, and by the Slovenian Research Agency (ARRS) under the Programme P1-0402.

## A Equivalence between the deterministic and nondeterministic dual gates

The validity of (52) can be demonstrated graphically. First we recall that  $P$  and  $Q$  are projectors, i.e.

$$\begin{array}{c} \circ \\ | \\ \circ \\ | \\ \circ \\ | \\ \circ \end{array} = \begin{array}{c} \circ \\ | \\ \circ \end{array}, \quad \begin{array}{c} \circ \\ | \\ \circ \\ | \\ \circ \\ | \\ \circ \\ | \\ \circ \end{array} = \begin{array}{c} \circ \\ | \\ \circ \\ | \\ \circ \end{array}. \quad (90)$$

Furthermore, all the local projectors commute and  $\hat{U}$  commutes with all the projectors with which it shares at most one site. Explicitly, this implies the following diagrams,

$$\begin{array}{c} \circ \\ | \\ \circ \\ | \\ \circ \\ | \\ \circ \\ | \\ \circ \end{array} = \begin{array}{c} \circ \\ | \\ \circ \\ | \\ \circ \\ | \\ \circ \end{array}, \quad \begin{array}{c} \circ \\ | \\ \circ \\ | \\ \circ \\ | \\ \circ \end{array} = \begin{array}{c} \circ \\ | \\ \circ \\ | \\ \circ \\ | \\ \circ \end{array}, \quad \begin{array}{c} \circ \\ | \\ \circ \\ | \\ \circ \\ | \\ \circ \end{array} = \begin{array}{c} \circ \\ | \\ \circ \\ | \\ \circ \\ | \\ \circ \end{array}, \quad \begin{array}{c} \circ \\ | \\ \circ \\ | \\ \circ \\ | \\ \circ \end{array} = \begin{array}{c} \circ \\ | \\ \circ \\ | \\ \circ \\ | \\ \circ \end{array}. \quad (91)$$

The last two properties needed for the proof are less trivial, but straightforward to check. Their diagrammatic form reads as

$$\begin{array}{c} \circ \\ | \\ \circ \\ | \\ \circ \\ | \\ \circ \\ | \\ \circ \end{array} = \begin{array}{c} \circ \\ | \\ \circ \\ | \\ \circ \\ | \\ \circ \end{array}, \quad \begin{array}{c} \circ \\ | \\ \circ \\ | \\ \circ \\ | \\ \circ \\ | \\ \circ \end{array} = \begin{array}{c} \circ \\ | \\ \circ \\ | \\ \circ \\ | \\ \circ \end{array}. \quad (92)$$

Using these equalities, we can now easily show the equivalence between (53) and (50). First we express the propagator  $\tilde{U}^e$  from (53) in terms of gates  $P$ ,  $Q$  and  $\hat{U}$ ,

$$\text{Diagrammatic equation (93)} \quad (93)$$

where we simplified the diagram by using the fact  $Q^2 = Q$  and commutation relations between the projectors and the gates (91). Using the second relation of (92) and moving around some of the commuting gates, we obtain the following,

$$\text{Diagrammatic equation (94)} \quad (94)$$

Now we use the first equality of (92) and reposition the commuting gates so that we can again apply the second equality of (92),

(95)

In the final step we again rearranged the operators to obtain  $\tilde{U}^e$  as defined in (50). The same reasoning applies to  $\tilde{U}^o$ , therefore (53) is equivalent to (50) and the dual propagation of RCA54 can be expressed in terms of local, deterministic 7-site gates on the reduced configuration space.

## B Dual circuit representation of correlation functions

A convenient way to show the equivalence between the diagrams in Eq. (60) is to interpret the circuits as a 2-dimensional vertex model. Each line segment is either in the state  $s = 0$  or  $s = 1$ , and the weights of vertices with large circles are given by the 3-site propagator  $U$  as,

$$\begin{array}{c} s_4 \\ | \\ \text{---} \bigcirc \text{---} \\ | \\ s_2 \end{array} \begin{array}{l} s_1 \\ \text{---} \\ s_3 \end{array} \equiv U_{(s_1, s_4, s_3), (s_1, s_2, s_3)} = \hat{U}_{(s_2, s_1, s_4), (s_2, s_3, s_4)}. \quad (96)$$

The small circles force all the incoming lines to be in the same state,

$$\begin{array}{c} s_k \\ | \\ \text{---} \bigcirc \text{---} \\ | \\ s_2 \quad s_3 \end{array} \equiv \delta_{s_1, s_2} \delta_{s_2, s_3} \cdots \delta_{s_{k-1}, s_k}, \quad (97)$$

where the weight is defined for any number  $k \geq 2$  of intersecting lines. In particular, for  $k = 2$  the diagram can be transformed into a straight line,

$$\text{---} \bigcirc \text{---} = \text{---}. \quad (98)$$

In this context, the one-site maximum entropy state  $\omega$  corresponds to the sum of the line segment in states 0 and 1. This implies that we can always attach or remove lines connected to the maximum entropy state from the small circle, as long as at the end at least one such lines remains,

$$\begin{array}{c} \bullet \\ | \\ \text{---} \bigcirc \text{---} \\ | \\ \bullet \end{array} = \begin{array}{c} \bullet \\ | \\ \text{---} \bullet \end{array}. \quad (99)$$

Using these relations, the equivalence of the diagrams from (60) can be recast as

$$(100)$$

This equality follows from the fact that the observables can be represented by diagonal one-site operators and can be therefore freely moved around the small circle,

$$(101)$$

## C Factorization of the equilibrium state and the local few-site relations

We start by explicitly expressing coefficients  $\alpha_{s_1 s_2 s_3}^{(l)}$ ,  $\beta_{s_1 s_2 s_3}^{(l)}$  that satisfy factorization condition in equation (75). Solving the first two factorization relations we obtain the following solution,

$$\begin{aligned} \alpha_{000} = \alpha_{100} = \alpha_{111} &= 1, & \alpha'_{000} = \alpha'_{001} = \alpha'_{111} &= 1, \\ \alpha_{001} = \alpha_{101} = \alpha_{110} &= \frac{\xi(\lambda + \omega - \xi\omega)}{\lambda + \xi - \xi\omega}, & \alpha'_{011} = \alpha'_{100} = \alpha'_{101} &= \frac{\omega(\lambda + \xi - \xi\omega)}{\lambda + \omega - \xi\omega}, \\ \alpha_{010} &= \frac{\lambda + \xi - \xi\omega}{\lambda + \omega - \xi\omega}, & \alpha'_{010} &= \frac{\lambda + \omega - \xi\omega}{\lambda + \xi - \xi\omega}, \\ \alpha_{011} &= \frac{\omega(\lambda + \xi - \xi\omega)^2}{(\lambda + \omega - \xi\omega)^2}, & \alpha'_{110} &= \frac{\xi(\lambda + \omega - \xi\omega)^2}{(\lambda + \xi - \xi\omega)^2}, \end{aligned} \quad (102)$$

where we can immediately see that one set of parameters is transformed into another one by exchanging  $\xi$  and  $\omega$ , and reversing the order of indices,

$$\alpha'_{s_1 s_2 s_3} = \alpha_{s_3 s_2 s_1} |_{\xi \leftrightarrow \omega}. \quad (103)$$

Similarly, solving the bottom two equations we obtain

$$\begin{aligned} \beta_{s_1 s_2 s_3} &= \alpha_{s_1 s_2 s_3}, & \beta'_{000} = \beta'_{001} = \beta'_{110} &= \alpha'_{000}, & \beta'_{011} &= \alpha'_{010}, \\ \beta'_{010} = \beta'_{100} = \beta'_{101} &= \alpha'_{100}, & \beta'_{111} &= \alpha'_{110}. \end{aligned} \quad (104)$$

To demonstrate how the factorization property of the equilibrium state enables us to formulate the few-site relations (76) and (77), we first introduce the following notation for the basis vectors from  $\mathbb{R}^{2^5}$ ,

$$\mathbf{e}_{s_1 s_2 s_3 s_4 s_5} = \mathbf{e}_{s_1} \otimes \mathbf{e}_{s_2} \otimes \mathbf{e}_{s_3} \otimes \mathbf{e}_{s_4} \otimes \mathbf{e}_{s_5}, \quad \mathbf{e}_0 = \begin{bmatrix} 1 \\ 0 \end{bmatrix}, \quad \mathbf{e}_1 = \begin{bmatrix} 0 \\ 1 \end{bmatrix}. \quad (105)$$



Now we can express the first identity from Eq. (76) in explicit component form as,

$$\begin{aligned}
& \sum_{s_1, s_2, s_3, s_4, s_5} \mathbf{e}_{s_1 s_2 s_3 s_4 s_5} \hat{U}_3 P_2 P_4 \cdot \langle l | W'_{s_3} S W'_{s_2} S W'_{s_1} \\
&= \sum_{s_1, s_2, s_3, s_4, s_5} \mathbf{e}_{s_1 s_2 s_3 s_4 s_5} \hat{U}_3 P_2 P_4 \cdot \alpha'_{s_3 s_2 s_1} \langle l | W'_{s_2} S W'_{s_1} \\
&= \sum_{s_1, s_2, s_3, s_4, s_5} \mathbf{e}_{s_1 s_2 s_3 s_4 s_5} P_2 P_4 \cdot (l | A_{s_2} B'_{s_3} A_{s_4} | r) \langle l | W'_{s_2} S W'_{s_1},
\end{aligned} \tag{106}$$

where to get from the first to the second line, we used the first of the factorization conditions (75). Note that  $\mathbf{B}$  and  $\mathbf{B}'$  satisfy an even stronger condition, where we can remove the sum over  $s_1$  and  $s_2$ . Namely,

$$\sum_{s_3, s_4, s_5} \mathbf{e}_{s_1 s_2 s_3 s_4 s_5} \hat{U}_3 P_2 P_4 \cdot \alpha'_{s_3 s_2 s_1} = \sum_{s_3, s_4, s_5} \mathbf{e}_{s_1 s_2 s_3 s_4 s_5} P_2 P_4 \cdot (l | A_{s_2} B'_{s_3} A_{s_4} | r). \tag{107}$$

## D Matrix-product form of multi-time correlation functions

To see that the MPS representation (89) is equivalent to time-states introduced in [31] we first explicitly spell out the matrices  $\tilde{A}_s, \tilde{A}'_s$  which by definition (87) take the following form,

$$\begin{aligned}
\tilde{A}_0 &= \begin{bmatrix} \alpha_{000} & \alpha_{001} & 0 & 0 \\ \alpha_{000} & \alpha_{001} & 0 & 0 \\ 0 & 0 & 0 & 0 \\ 0 & 0 & 0 & 0 \end{bmatrix}, & \tilde{A}_1 &= \begin{bmatrix} 0 & 0 & 0 & 0 \\ 0 & 0 & 0 & 0 \\ 0 & 0 & 0 & \alpha_{000} + \alpha_{001} \\ 0 & 0 & \alpha_{000} + \alpha_{001} & 0 \end{bmatrix}, \\
\tilde{A}'_0 &= \begin{bmatrix} \alpha'_{000} & 0 & \alpha'_{100} & 0 \\ 0 & 0 & 0 & 0 \\ \alpha'_{000} & 0 & \alpha'_{100} & 0 \\ 0 & 0 & 0 & 0 \end{bmatrix}, & \tilde{A}'_1 &= \begin{bmatrix} 0 & 0 & 0 & 0 \\ 0 & 0 & 0 & \alpha'_{000} + \alpha'_{100} \\ 0 & 0 & 0 & 0 \\ 0 & 0 & \alpha'_{000} + \alpha'_{100} & 0 \end{bmatrix},
\end{aligned} \tag{108}$$

while the boundary vectors ( $\langle \tilde{L} |$  and  $| \tilde{R} \rangle$ ) that solve equation (88) can be after some straightforward algebraic manipulation expressed as

$$\begin{aligned}
\langle \tilde{L} | &= \frac{\alpha'_{000} + \alpha'_{100}}{1 + \frac{\alpha_{001}}{\alpha_{000} + \alpha_{001}} + \frac{\alpha'_{100}}{\alpha'_{000} + \alpha'_{100}}} \left[ \frac{\alpha'_{000}}{\alpha'_{000} + \alpha'_{100}} \quad \frac{\alpha'_{100}}{\alpha'_{000} + \alpha'_{100}} \quad \frac{\alpha'_{100}}{\alpha'_{000} + \alpha'_{100}} \quad \frac{\alpha_{001}}{\alpha_{000} + \alpha_{001}} \right], \\
| \tilde{R} \rangle &= \frac{1}{\alpha'_{000} + \alpha'_{100}} [1 \quad 1 \quad 1 \quad 1]^T.
\end{aligned} \tag{109}$$

Additionally, we note that the product  $(\alpha_{000} + \alpha_{001})(\alpha'_{000} + \alpha'_{100})$  is equal to the leading eigenvalue  $\lambda$  of  $(W'_0 + W'_1)(W_0 + W_1)$ ,

$$\lambda = (\alpha_{000} + \alpha_{001})(\alpha'_{000} + \alpha'_{100}). \tag{110}$$

Equipped by these relations, it is easy to see that it is possible to introduce linear maps  $Q, U, V$ ,

$$U = \begin{bmatrix} 1 & 0 & 0 & -\frac{\alpha_{001}}{\alpha_{000}} \\ 1 & 0 & 0 & 1 \\ 0 & 0 & 1 & 0 \\ 0 & 1 & 0 & 0 \end{bmatrix}, \quad V = \begin{bmatrix} 1 & 0 & 0 & -\frac{\alpha'_{100}}{\alpha'_{000}} \\ 0 & 0 & 1 & 0 \\ 1 & 0 & 0 & 1 \\ 0 & 1 & 0 & 0 \end{bmatrix}, \quad Q = \begin{bmatrix} 1 & 0 & 0 & 0 \\ 0 & 1 & 0 & 0 \\ 0 & 0 & 1 & 0 \end{bmatrix}, \tag{111}$$

so that the following holds for any  $s_1, s_2 \in \{0, 1\}$ ,

$$\begin{aligned} \tilde{A}_{s_1} U Q^T Q U^{-1} \tilde{A}'_{s_2} &= \tilde{A}_{s_1} \tilde{A}'_{s_2}, & \tilde{A}'_{s_1} V Q^T Q V^{-1} \tilde{A}_{s_2} &= \tilde{A}'_{s_1} \tilde{A}_{s_2}, \\ ((\tilde{L} | V Q^T Q V^{-1} \tilde{A}_{s_1} &= ((\tilde{L} | \tilde{A}_{s_1}, & \tilde{A}'_{s_1} V Q^T Q V^{-1} | \tilde{R})) &= \tilde{A}'_{s_1} | \tilde{R})). \end{aligned} \quad (112)$$

This implies that the state (89) can be equivalently represented by an MPS with a 3-dimensional auxiliary space

$$\mathbf{q} = \langle x_L | \mathbf{X}_1 \mathbf{X}'_2 \mathbf{X}_3 \cdots \mathbf{X}'_{2m} | x_R \rangle, \quad (113)$$

where the new matrices  $X_s, X'_s$  and boundary vectors  $\langle x_L |, | x_R \rangle$  are defined as

$$\begin{aligned} X_s &= \frac{1}{\alpha_{000} + \alpha_{001}} Q V^{-1} \tilde{A}_s U Q^T, & X'_s &= \frac{1}{\alpha'_{000} + \alpha'_{001}} Q V^{-1} \tilde{A}'_s U Q^T, \\ \langle x_L | &= \frac{1}{\alpha'_{000} + \alpha'_{100}} ((\tilde{L} | V Q^T, & | x_R \rangle &= (\alpha'_{000} + \alpha'_{100}) Q V^{-1} | \tilde{R})), \end{aligned} \quad (114)$$

which implies the following explicit form,

$$\begin{aligned} X_0 &= \begin{bmatrix} \frac{\alpha'_{000}}{\alpha'_{000} + \alpha'_{100}} & 0 & 0 \\ 0 & 0 & 0 \\ 1 & 0 & 0 \end{bmatrix}, & X_1 &= \begin{bmatrix} 0 & \frac{\alpha'_{100}}{\alpha'_{000} + \alpha'_{100}} & 0 \\ 0 & 0 & 1 \\ 0 & 0 & 0 \end{bmatrix}, \\ X'_0 &= \begin{bmatrix} \frac{\alpha_{000}}{\alpha_{000} + \alpha_{001}} & 0 & 0 \\ 0 & 0 & 0 \\ 1 & 0 & 0 \end{bmatrix}, & X'_1 &= \begin{bmatrix} 0 & \frac{\alpha_{100}}{\alpha_{000} + \alpha_{001}} & 0 \\ 0 & 0 & 1 \\ 0 & 0 & 0 \end{bmatrix}, \\ \langle x_L | &= \frac{1}{1 + \frac{\alpha_{001}}{\alpha_{000} + \alpha_{001}} + \frac{\alpha'_{100}}{\alpha'_{000} + \alpha'_{100}}} \left[ 1 \quad \frac{\alpha_{001}}{\alpha_{000} + \alpha_{001}} \quad \frac{\alpha'_{100}}{\alpha'_{000} + \alpha'_{100}} \right], \\ | x_R \rangle &= [1 \quad 1 \quad 1]^T. \end{aligned} \quad (115)$$

Finally, to see that this parametrization coincided with the MPS from Ref. [31], one needs to only express parameters  $\frac{\alpha_{001}}{\alpha_{000} + \alpha_{001}}$  and  $\frac{\alpha'_{100}}{\alpha'_{000} + \alpha'_{100}}$  in terms of  $\xi, \omega$  and  $\lambda$ .

## References

- [1] R. J. Baxter, *Exactly solved models in statistical mechanics*, Elsevier (2016).
- [2] B. Sutherland, *Beautiful models*, World Scientific Publishing Company (2004).
- [3] P. Calabrese, F. H. L. Essler and G. Mussardo, *Introduction to ‘quantum integrability in out of equilibrium systems’*, J. Stat. Mech. **2016**(6), 064001 (2016), doi:10.1088/1742-5468/2016/06/064001.
- [4] P. Calabrese and J. Cardy, *Quantum quenches in 1+1 dimensional conformal field theories*, J. Stat. Mech. **2016**(6), 064003 (2016), doi:10.1088/1742-5468/2016/06/064003.
- [5] O. A. Castro-Alvaredo, B. Doyon and T. Yoshimura, *Emergent hydrodynamics in integrable quantum systems out of equilibrium*, Phys. Rev. X **6**, 041065 (2016), doi:10.1103/PhysRevX.6.041065.

- [6] B. Bertini, M. Collura, J. De Nardis and M. Fagotti, *Transport in out-of-equilibrium xxz chains: Exact profiles of charges and currents*, Phys. Rev. Lett. **117**, 207201 (2016), doi:10.1103/PhysRevLett.117.207201.
- [7] A. Nahum, J. Ruhman, S. Vijay and J. Haah, *Quantum entanglement growth under random unitary dynamics*, Phys. Rev. X **7**, 031016 (2017), doi:10.1103/PhysRevX.7.031016.
- [8] A. Nahum, S. Vijay and J. Haah, *Operator spreading in random unitary circuits*, Phys. Rev. X **8**, 021014 (2018), doi:10.1103/PhysRevX.8.021014.
- [9] C. W. von Keyserlingk, T. Rakovszky, F. Pollmann and S. L. Sondhi, *Operator hydrodynamics, otocs, and entanglement growth in systems without conservation laws*, Phys. Rev. X **8**, 021013 (2018), doi:10.1103/PhysRevX.8.021013.
- [10] A. Chan, A. De Luca and J. T. Chalker, *Solution of a minimal model for many-body quantum chaos*, Phys. Rev. X **8**, 041019 (2018), doi:10.1103/PhysRevX.8.041019.
- [11] B. Bertini, P. Kos and T. Prosen, *Exact correlation functions for dual-unitary lattice models in 1+ 1 dimensions*, Phys. Rev. Lett. **123**, 210601 (2019), doi:10.1103/PhysRevLett.123.210601.
- [12] J. Avan, V. Caudrelier, A. Doikou and A. Kundu, *Lagrangian and hamiltonian structures in an integrable hierarchy and space-time duality*, Nucl. Phys. B **902**, 415 (2016), doi:10.1016/j.nuclphysb.2015.11.024.
- [13] I. Findlay, *A dual construction of the isotropic landau–lifshitz model*, Physica D **398**, 13 (2019), doi:10.1016/j.physd.2019.06.003.
- [14] A. Doikou, I. Findlay and S. Sklaveniti, *Time-like boundary conditions in the nls model*, Nucl. Phys. B **941**, 361 (2019), doi:10.1016/j.nuclphysb.2019.02.022.
- [15] B. Gutkin, P. Braun, M. Akila, D. Waltner and T. Guhr, *Local correlations in dual-unitary kicked chains*, arXiv:2001.01298 (2020).
- [16] B. Bertini, P. Kos and T. Prosen, *Entanglement spreading in a minimal model of maximal many-body quantum chaos*, Phys. Rev. X **9**, 021033 (2019), doi:10.1103/PhysRevX.9.021033.
- [17] L. Piroli, B. Bertini, J. I. Cirac and T. Prosen, *Exact dynamics in dual-unitary quantum circuits*, Phys. Rev. B **101**, 094304 (2020), doi:10.1103/PhysRevB.101.094304.
- [18] S. Gopalakrishnan and A. Lamacraft, *Unitary circuits of finite depth and infinite width from quantum channels*, Phys. Rev. B **100**(6) (2019), doi:10.1103/physrevb.100.064309.
- [19] B. Bertini, P. Kos and T. Prosen, *Operator entanglement in local quantum circuits i: Maximally chaotic dual-unitary circuits*, arXiv:1909.07407 (2019).
- [20] B. Bertini, P. Kos and T. Prosen, *Operator entanglement in local quantum circuits ii: Solitons in chains of qubits*, arXiv:1909.07410 (2019).
- [21] P. W. Claeys and A. Lamacraft, *Maximum velocity quantum circuits*, arXiv:2003.01133 (2020).

- [22] Ž. Krajnik and T. Prosen, *Kardar-parisi-zhang physics in integrable rotationally symmetric dynamics on discrete space-time lattice*, arXiv:1909.03799 (2019).
- [23] Ž. Krajnik, E. Ilievski and T. Prosen, *Integrable matrix models in discrete space-time*, arXiv:2003.05957 (2020).
- [24] A. Bobenko, M. Bordemann, C. Gunn and U. Pinkall, *On two integrable cellular automata*, Commun. Math. Phys. **158**(1), 127 (1993), doi:10.1007/BF02097234.
- [25] S. Takesue, *Reversible cellular automata and statistical mechanics*, Phys. Rev. Lett. **59**, 2499 (1987), doi:10.1103/PhysRevLett.59.2499.
- [26] T. Prosen and C. Mejía-Monasterio, *Integrability of a deterministic cellular automaton driven by stochastic boundaries*, J. Phys. A: Math. Theor. **49**(18), 185003 (2016), doi:10.1088/1751-8113/49/18/185003.
- [27] A. Inoue and S. Takesue, *Two extensions of exact nonequilibrium steady states of a boundary-driven cellular automaton*, J. Phys. A: Math. Theor. **51**(42), 425001 (2018), doi:10.1088/1751-8121/aadc29.
- [28] T. Prosen and B. Buča, *Exact matrix product decay modes of a boundary driven cellular automaton*, J. Phys. A: Math. Theor. **50**(39), 395002 (2017), doi:10.1088/1751-8121/aa85a3.
- [29] B. Buča, J. P. Garrahan, T. Prosen and M. Vanicat, *Exact large deviation statistics and trajectory phase transition of a deterministic boundary driven cellular automaton*, Phys. Rev. E **100**, 020103 (2019), doi:10.1103/PhysRevE.100.020103.
- [30] K. Klobas, M. Medenjak, T. Prosen and M. Vanicat, *Time-dependent matrix product ansatz for interacting reversible dynamics*, Commun. Math. Phys. **371**(2), 651 (2019), doi:10.1007/s00220-019-03494-5.
- [31] K. Klobas, M. Vanicat, J. P. Garrahan and T. Prosen, *Matrix product state of multi-time correlations*, arXiv:1912.09742 (2019).
- [32] S. Gopalakrishnan, *Operator growth and eigenstate entanglement in an interacting integrable floquet system*, Phys. Rev. B **98**, 060302 (2018), doi:10.1103/PhysRevB.98.060302.
- [33] S. Gopalakrishnan, D. A. Huse, V. Khemani and R. Vasseur, *Hydrodynamics of operator spreading and quasiparticle diffusion in interacting integrable systems*, Phys. Rev. B **98**, 220303 (2018), doi:10.1103/PhysRevB.98.220303.
- [34] A. J. Friedman, S. Gopalakrishnan and R. Vasseur, *Integrable many-body quantum floquet-thouless pumps*, Phys. Rev. Lett. **123**, 170603 (2019), doi:10.1103/PhysRevLett.123.170603.
- [35] V. Alba, J. Dubail and M. Medenjak, *Operator entanglement in interacting integrable quantum systems: the case of the rule 54 chain*, Phys. Rev. Lett. **122**, 250603 (2019), doi:10.1103/PhysRevLett.122.250603.